JAMECH
Vol. 46, No. 1, January 2015, pp 1- 12

Nonlinear Flow-Induced Flutter Instability of Double CNTs Using Reddy Beam Theory

A. Ghorbanpour Arani [1*], S. Amir [2], A. Karamali Ravandi [3]

1. Professor, Faculty of Mechanical Engineering, University of Kashan, Kashan, Iran

2. Assistant of professor, Faculty of Mechanical Engineering, University of Kashan, Kashan, Iran

3. MS Graduate, Faculty of Mechanical Engineering, University of Kashan, Kashan, Iran

Received 25 August 2014; Accepted 7 October 2014

Abstract

In this study, nonlocal nonlinear instability and the vibration of a double carbon nanotube (CNT) system have been investigated. The Visco-Pasternak model is used to simulate the elastic medium between nanotubes, on which the effect of the spring, shear and damping of the elastic medium is considered. Both of the CNTs convey a viscose fluid and a uniform longitudinal magnetic field is applied to them. The fluid velocity is modified by small-size effects on the bulk viscosity and the slip boundary conditions of nano flow through the Knudsen number (*Kn*). Using von Kármán geometric nonlinearity, Hamilton's principle and considering longitudinal magnetic field, the nonlinear higher order governing equations for Reddy beam (*RB*) theory are derived. The differential quadrature method (DQM) is used to obtain the nonlinear frequency and critical fluid velocity (CFV) of the fluid conveying a coupled system. A detailed parametric study is conducted, focusing on the effects of parameters such as magnetic field strength, Knudsen number, aspect ratio, small scale and elastic foundation on the in-phase and out-of-phase vibration of the nanotube. The results indicate that the natural frequency and the critical fluid velocity of double bonded Reddy beams increase with an increase in the longitudinal magnetic field and elastic medium module. Furthermore, the results of this study can be useful for designing and manufacturing micro/nano- double-mechanical systems in advanced mechanics applications by controlling nonlinear frequency with an applied magnetic field.

Keywords: *conveying fluid, double nanosystem, flutter phenomena, nonlinear vibration, nonlocal theory, Reddy beam.*

1. Introduction

Beam models are the most important and applicable theories for simulating many structures. They are widely used in some branches of engineering sciences such as mechanical and civil engineering. The study of the behaviour of beam structures has been lionized by many researchers during recent

[*] Corresponding Author. Tel.: +98 31 55912450
Email Address: aghorban@kashanu.ac.ir

years. A large number of studies have looked at the vibration and buckling analysis of beams that do and do not convey fluid. Reddy [1] proposed nonlocal theories for the bending, buckling and vibration of beams using nonlocal elasticity theory. He reported nonlocal governing equations of different beams such as the Euler-Bernoulli beam (EBB), the Timoshenko beam (TB) and the Reddy beam (RB) theories. Reddy and Wang [2] studied the dynamic characteristics of fluid-conveying EBB and TB using finite element models. Lin and Qiao [3] investigated the vibration and instability of CNTs conveying fluid where the DQM is utilized to discretize the equations of motion. They showed that a couple mode flutter occurs at a higher flow velocity and the resonant frequencies were obtained by solving a generalized eigenvalue problem. Chang [4] presented the thermal-mechanical vibration and instability of a fluid-conveying single-walled carbon nanotube (SWCNT) embedded in an elastic medium based on nonlocal elasticity theory. He found that the fundamental natural frequency for the SWCNT decreases as the nonlocal parameter increases. Furthermore, both the fundamental natural frequency and critical flow velocity increase as the elastic medium constantly increases. Ghorbanpour Arani et al. [5] investigated the nonlinear nonlocal vibration of an embedded double-walled carbon nanotube (DWCNT) conveying fluid using a shell model. According to their study, the critical flow velocity of DWCNT is inversely related to the nonlocal parameter.

Double systems have received considerable attention from researchers recently. Ghorbanpour Arani and Amir [6] analysed the electro-thermal vibration behaviour of a double BNNT system that is coupled by a Visco-Pasternak medium using EBB theory. Two BNNTs were placed in uniform temperature and electric fields, the latter being applied through electrodes attached at both ends. Murmu and Adhikari [7] studied the axial instability of double-nanobeam-systems. Their results demonstrate that increasing the stiffness of the coupling elastic medium in a double-nanobeam-system reduces the small scale effects during the out-of-phase buckling modes. Nonlocal effects in the forced vibration of an elastically connected double-CNT system under a moving nanoparticle were studied by Simsek [8]. He showed that the velocity of the nanoparticle and the stiffness of the elastic layer have significant effects on the dynamic behaviour of DWCNT. Murmu and Adhikari [9] presented nonlocal elasticity-based vibration of initially pre-stressed coupled nanobeam systems. Based on their obtained results, it appears that there is a considerable difference by which the pre-load affects the nonlocal frequency in the in-phase type and out-of-phase type vibration modes of nonlocal double-nanobeam-systems.

Among all the beam theories, there are few published papers about RB in the literature. Hence, in this study, our aim is to study the vibration of a double CNT system based on nonlocal elasticity theory where both of them are simulated as an RB model and are considered to be fluid-conveyed. The CNTs are coupled together via a Visco-Pasternak medium and the whole system is placed in a uniform magnetic field. Higher-order equations of motion have been derived based on Hamilton's principle and DQM is applied to solve them. Finally, the influences of various factors such as aspect ratio, elastic medium and magnetic field on the frequency response of the system are studied. The results show significant effects of nonlocal parameters, magnetic field and the velocity of the fluid flow on the fundamental natural frequency of the system.

2. Modelling SWCNT Coupled System

Figure 1 illustrates a SWCNT coupled system conveying fluid surrounded by a Visco-Pasternak foundation under a longitudinal magnetic field. The boundary conditions are assumed as being clamped-clamped for both nanotubes. In this investigation, nanotubes are simulated by RB where the displacement field along three directions of (x, y, z) in this model is given respectively as follows [1]:

$$\begin{aligned} u_1 &= u(x,t) + z\varphi(x,t) - c_1 z^3\left(\varphi(x,t) + \frac{\partial w(x,t)}{\partial x}\right) \\ u_2 &= 0 \\ u_3 &= w(x,t) \end{aligned} \tag{1}$$

where u and w denote the axial and transverse

displacements of a point located on the neutral axis of the beam, respectively, and ϕ is the rotation of the cross section.

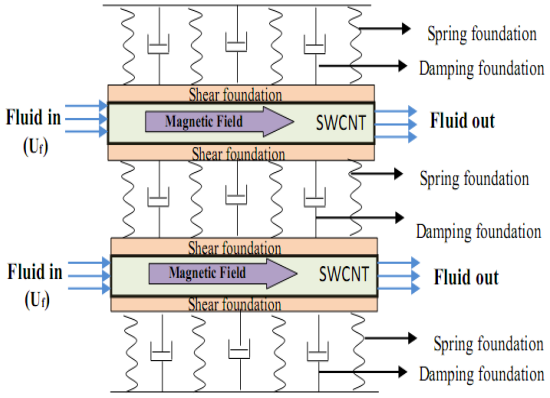

Fig. 1. Schematic of a double CNT system conveying fluid, under a magnetic field and a Visco-Pasternak foundation

The linear kinematic relations for the RB model are [1]:

$$\varepsilon_{xx} = \frac{\partial u}{\partial x} + z\left(1 - c_1 z^2\right)\frac{\partial \varphi}{\partial x} - c_1 z^3 \frac{\partial^2 w}{\partial x^2}$$
$$2\varepsilon_{xz} = \gamma_{xz} = \left(1 - c_2 z^2\right)\left(\frac{\partial w}{\partial x} + \varphi\right) \quad (2)$$

where

$$C_1 = 4/3h^2 \ , \quad C_2 = 4/h^2 \quad (3)$$

h is the cross section height of the beam.

The stress-strain relationship of anelastic structure is expressed generally as:

$$\{\sigma\} = [C]\{\varepsilon\} \quad (4)$$

where $\{\sigma\}$ and $\{\varepsilon\}$ are classical stress and strain vectors, respectively and $[C]$ is expressed as an elastic stiffness matrix. Considering one-dimensional elasticity, Equation (4) may be reduced to [1]:

$$\sigma_{xx} = c_{11}\varepsilon_{xx} \ , \quad \sigma_{xz} = c_{55}\varepsilon_{xz} \quad (5)$$

where c_{11} and c_{55} are linear elastic constants.

In this study, Hamilton's principle is used to obtain equations of motion. Before utilizing this principle, the following preliminary functions must be calculated:

a) Strain energy

$$U_s = \frac{1}{2}\int_0^L \int_A \left(\sigma_{xx}\varepsilon_{xx} + 2\sigma_{xz}\varepsilon_{xz}\right) dA\,dx \quad (6)$$

where A is an area of the cross section of the nanotube. Equation (2) must be substituted in this equation. It should be noted that by simplifying Equation (6), we will encounter definitions of stress and couple resultants as follows:

$$N = \int_A \sigma_{xx} dA \ , \ M = \int_A z\,\sigma_{xx} dA$$
$$R = \int_A z^2 \sigma_{xz} dA \ , \ P = \int_A z^3 \sigma_{xx} dA \quad (7)$$
$$Q = \int_A \sigma_{xz} dA$$

b) Kinetic energy

The total kinetic energy of this double-system is divided into two parts: the kinetic energy of the nanotube and the kinetic energy of the fluid. Their values have been calculated as:

$$K_{tube} = \frac{1}{2}\rho_t \int_0^L \int_A \left[\left(\frac{\partial u_1}{\partial t}\right)^2 + \left(\frac{\partial u_3}{\partial t}\right)^2\right] dA\,dx \quad (8)$$

where ρ_t is the density of the nanotube. The values of the axial and lateral displacements are replaced by their equivalences where defined in Equation (1). On the other hand, the velocity vector of the flow $\left(\vec{V} = (V_x, V_z)\right)$ through the nanotube in the two-dimensional beam model is the relative velocity of the fluid and nanotube. This vector was introduced by Reddy and Wang [2] at a macro scale and then used by Kuang et al. [10] at a nano scale. This vector can be expressed as:

$$V_x = \frac{\partial u_1}{\partial t} + V_{mf}\cos\theta$$
$$V_z = \frac{\partial u_3}{\partial t} - V_{mf}\sin\theta \quad (9)$$

where $\theta = -\frac{\partial w}{\partial x}$ and V_{mf} is the modified fluid velocity using Knudsen number. According to the above relations, the kinetic energy of the fluid flow is given as:

$$K_{fluid} = \frac{1}{2}\rho_f \int_0^L \left(V_x^2 + V_z^2\right) dA_f\,dx \quad (10)$$

where ρ_f represents the density of the fluid.

c) External works

The external works applied to the system are due to the Visco-Pasternak foundation, the magnetic field and the centrifugal force of the fluid. The effects of the elastic medium on the nanotubes are considered as [6]:

$$\begin{aligned} F_{vp-1} &= K_w\left(w_1 - w_2\right) - G_p\nabla^2\left(w_1 - w_2\right) + \\ &\quad c_v\left(\dot{w}_1 - \dot{w}_2\right) + K_w w_1 - G_p\nabla^2 w_1 + c_v\dot{w}_1 \\ F_{vp-2} &= K_w\left(w_2 - w_1\right) - G_p\nabla^2\left(w_2 - w_1\right) + \\ &\quad c_v\left(\dot{w}_2 - \dot{w}_1\right) + K_w w_2 - G_p\nabla^2 w_2 + c_v\dot{w}_2 \end{aligned} \tag{11}$$

where K_w, G_P and c_v are the spring, shear and damping modulus, respectively. The Lorentz force induced by the magnetic field is given by [11]:

$$F_L = \eta^m A H_x^2 \frac{\partial^2 w}{\partial x^2} \tag{12}$$

where η^m and H_x are the magnetic field permeability and magnetic field vector component along *x* direction, respectively.

Therefore, the work done by the Visco-Pasternak foundation and the magnetic field is:

$$\begin{aligned} W_{vp-1} &= \frac{1}{2}\int_0^L\left(-F_{vp-1}W_1\right)dx \quad , \\ W_{L-1} &= \frac{1}{2}\int_0^L\left(-F_L W_1\right)dx \end{aligned} \tag{13}$$

The external force due to the centrifugal force of the fluid is expressed as [2]:

$$w_f = -\int_0^L\int_{A_f}\left\{\begin{array}{l}\left(m_f V_{mf}^2\frac{\partial^2 w_1}{\partial x^2}\cos\theta\right)w_1 + \\ \left(m_f V_{mf}^2\frac{\partial^2 w_1}{\partial x^2}\sin\theta\right)u_1\end{array}\right\}dA_f\,dx \tag{14}$$

where $m_f = \rho_f A_f$ is the mass density of the fluid and subscript f refers to the fluid.

d) Viscosity of the fluid

To evaluate the viscosity effect for this system, the Navier-Stokes equation can be used [12]:

$$\rho_f\frac{d\vec{V}}{dt} = -\nabla P + \mu\nabla^2\vec{V} \tag{15}$$

where $\frac{d}{dt}$ denotes the material derivative and is defined as follows:

$$\frac{d}{dt} = \left[\frac{\partial}{\partial t} + V_{mf}\frac{\partial}{\partial x}\right] \tag{16}$$

Substituting the fluid velocity from Equation (9) and then Equation (16) in Equation (15), applying surface integrals to the above equation, viscosity terms were elicited and added to the equation of motion.

The governing equations for the conventional fluid-structure interaction problems have been derived by the assumption of no-slip boundary conditions. To implement slip boundary conditions, considering a fully developed flow for a Newtonian fluid with a constant pressure gradient irrespective of gravitational body force, the Navier-Stokes equations may be given as:

$$\rho_f\frac{d\vec{V}}{dt} = -\nabla P + \mu_e\nabla^2\vec{V} \tag{17}$$

where μ_e is effective viscosity in which the following relation has been suggested for the viscosity of fluid as a function of Kn [13]:

$$\mu_e = \mu_0\left(\frac{1}{1+bKn}\right) \tag{18}$$

where μ_0 is the bulk viscosity and b is a coefficient and can vary from zero to a constant value and their values can be found in [13]. On the other hand, the velocity correction factor is [14]:

$$VCF = \frac{V_{mf}}{V_{avg-no\,slip}} = \frac{1}{1+b\,Kn\left(1+4\left(\frac{2-\sigma_v}{\sigma_v}\right)\left(\frac{Kn}{1+Kn}\right)\right)} \tag{19}$$

σ_v is the tangential moment accommodation coefficient and for most practical problems it is considered as being 0.7. Therefore, the motion equations of the embedded coupled SWCNT conveying viscose fluid can be derived by Hamilton's principle as follows:

$$\int_0^t\delta\left(K_{tube} + K_{fluid} - \left(U_s - W_s - W_{vis\,cosity}\right)\right)dt = 0 \tag{20}$$

where W_s denotes the total work done by the Lorentz force, the Visco-Pasternak foundation and the centrifugal force of the fluid. Integrating Equation (20) by parts and setting the coefficient of mechanical to zero leads to the following local motion equations for nanotube No. 1 and for nanotube No. 2 the notations 1 and 2 are replaced to gather.

(u_1, φ_1, w_1):

δu_1:

$$\frac{\partial N}{\partial x} - \left[\left(m_0 + mf_0 \right) \frac{\partial^2 u_1}{\partial t^2} + mf_0 V_{mf} \frac{\partial^2 w_1}{\partial x \partial t} \sin\theta + mf_0 V_{mf}{}^2 \frac{\partial^2 w_1}{\partial x^2} \sin\theta - \mu_e A_f \frac{\partial^3 u_1}{\partial x^2 \partial t} - \right. \tag{21}$$

$$\left. \mu_e A_f V_{mf} \frac{\partial^3 w_1}{\partial x^3} \sin\theta + \mu_e A_f V_{mf} \left(\frac{\partial^2 w_1}{\partial x^2} \right)^2 \cos\theta \right] = 0$$

$\delta \varphi_1$:

$$-\frac{\partial \hat{M}}{\partial x} - \hat{Q} - \left[\hat{m}_2 \frac{\partial^2 \varphi_1}{\partial t^2} - c_1 \hat{m}_4 \left(\frac{\partial^2 \varphi_1}{\partial t^2} + \frac{\partial^3 w_1}{\partial x \partial t^2} \right) - 2c_1 mf_4 \frac{\partial^2 \varphi_1}{\partial t^2} + c_1^2 mf_6 \left(\frac{\partial^2 \varphi_1}{\partial t^2} + \frac{\partial^3 w_1}{\partial x \partial t^2} \right) + \right. \tag{22}$$

$$\left. c_1 mf_4 \frac{\partial^3 w_1}{\partial x \partial t^2} + mf_2 \frac{\partial^2 \varphi_1}{\partial t^2} \right] = 0$$

δw_1:

$$\frac{\partial \hat{Q}}{\partial x} + C_1 \frac{\partial^2 P}{\partial x^2} - \left[\left(m_0 + mf_0 \right) \frac{\partial^2 w_1}{\partial t^2} + c_1 m_4 \frac{\partial^3 \varphi_1}{\partial x \partial t^2} - c_1^2 m_6 \left(\frac{\partial^3 \varphi_1}{\partial x \partial t^2} + \frac{\partial^4 w_1}{\partial x^2 \partial t^2} \right) + mf_0 V_{mf} \frac{\partial^2 u_1}{\partial x \partial t} \sin\theta - \right.$$

$$mf_0 V_{mf} \frac{\partial u_1}{\partial t} \frac{\partial^2 w_1}{\partial x^2} \cos\theta + c_1 mf_4 \frac{\partial^3 \varphi_1}{\partial x \partial t^2} - c_1^2 mf_6 \frac{\partial^3 \varphi_1}{\partial x \partial t^2} - c_1^2 mf_6 \frac{\partial^4 w_1}{\partial x^2 \partial t^2} + 2mf_0 V_{mf} \frac{\partial^2 w_1}{\partial x \partial t} \cos\theta + \tag{23}$$

$$mf_0 V_{mf} \frac{\partial w_1}{\partial t} \frac{\partial^2 w_1}{\partial x^2} \sin\theta + 4k_w w_1 - 4G_p \frac{\partial^2 w_1}{\partial x^2} - k_w w_2 + G_p \frac{\partial^2 w_2}{\partial x_2} - c_v \frac{\partial w_2}{\partial t} - c_v \frac{\partial w_1}{\partial t} +$$

$$\left. mf_0 V_{mf}{}^2 \frac{\partial^2 w_1}{\partial x^2} \cos\theta + 2\eta A H_x^2 \frac{\partial^2 w_1}{\partial x^2} - \mu_e A_f V_{mf} \frac{\partial^3 w_1}{\partial x^3} - \mu_e A_f V_{mf} \frac{\partial^3 w_1}{\partial x^2 \partial t} - \mu_e A_f V_{mf} \left(\frac{\partial^2 w_1}{\partial x^2} \right)^2 \sin\theta \right] = 0$$

3. Nonlocal Continuum Model for RB

According to the nonlocal elasticity theory proposed by Eringen [15], the stress field at a specific point x in an elastic continuum not only depends on the strain field at the same point but also on the strain at all other points of the body.

The constitutive equation of the nonlocal elasticity becomes:

$$\left(1 - \left(e_0 a\right)^2 \nabla^2\right) \sigma = \tau \tag{24}$$

where ∇^2 is the Laplacian operator, σ and τ are nonlocal and local stress fields, respectively. The nonlocal constitutive Equation (24) has been widely used for the study of micro- and nanostructure elements. Therefore, non-zero nonlocal stresses for the nanotube structures are outlined as [1]:

$$\begin{aligned}
&N - \mu \frac{\partial^2 N}{\partial x^2} = EA\, \varepsilon_{xx}^0 \ , \\
&M - \mu \frac{\partial^2 M}{\partial x^2} = EI\, \kappa + EJ\, \rho \ , \\
&P - \mu \frac{\partial^2 P}{\partial x^2} = EJ\, \kappa + E\, \kappa\rho \ , \\
&Q - \mu \frac{\partial^2 Q}{\partial x^2} = GA\, \gamma + GI\, \beta \ , \\
&R - \mu \frac{\partial^2 R}{\partial x^2} = GI\, \gamma + GJ\, \beta \ , \\
&\left(A, I, J, K\right) = \int_A \left(1, z^2, z^4, z^6\right) dA
\end{aligned} \tag{25}$$

Using relations (25), nonlocal forms of Equations (21-23) are obtained as:

δu_1 :

$$EA\frac{\partial^2 u_1}{\partial x^2}-\left(1-\mu\nabla^2\right)\times\left[\left(m_0+mf_0\right)\frac{\partial^2 u_1}{\partial t^2}+mf_0V_{mf}\frac{\partial^2 w_1}{\partial x\,\partial t}\sin\theta+mf_0V_{mf}{}^2\frac{\partial^2 w_1}{\partial x^2}\sin\theta-\mu_eA_f\frac{\partial^3 u_1}{\partial x^2\partial t}-\right.$$
$$\left.\mu_eA_fV_{mf}\frac{\partial^3 w_1}{\partial x^3}\sin\theta+\mu_eA_fV_{mf}\left(\frac{\partial^2 w_1}{\partial x^2}\right)^2\cos\theta\right]=0 \tag{26}$$

$\delta\phi_1$:

$$E\hat{I}\frac{\partial^2\varphi_1}{\partial x^2}-c_1E\hat{J}\left(\frac{\partial^2\varphi_1}{\partial x^2}+\frac{\partial^3 w_1}{\partial x^3}\right)-G\tilde{A}\left(\varphi_1+\frac{\partial w_1}{\partial x}\right)-\left(1-\mu\nabla^2\right)\left[\hat{m}_2\frac{\partial^2\varphi_1}{\partial t^2}-c_1\hat{m}_4\left(\frac{\partial^2\varphi_1}{\partial t^2}+\frac{\partial^3 w_1}{\partial x\,\partial t^2}\right)-\right.$$
$$\left.2c_1mf_4\frac{\partial^2\varphi_1}{\partial t^2}+c_1^2mf_6\left(\frac{\partial^2\varphi_1}{\partial t^2}+\frac{\partial^3 w_1}{\partial x\,\partial t^2}\right)+c_1mf_4\frac{\partial^3 w_1}{\partial x\,\partial t^2}+mf_2\frac{\partial^2\varphi_1}{\partial t^2}\right]=0 \tag{27}$$

δw_1 :

$$G\tilde{A}\left(\frac{\partial\varphi_1}{\partial x}+\frac{\partial^2 w_1}{\partial x^2}\right)+c_1\left[EJ\frac{\partial^3\varphi_1}{\partial x^3}-c_1EK\left(\frac{\partial^3\varphi_1}{\partial x^3}+\frac{\partial^4 w_1}{\partial x^4}\right)\right]-\left(1-\mu\nabla^2\right)\left[\left(m_0+mf_0\right)\frac{\partial^2 w_1}{\partial t^2}+c_1m_4\frac{\partial^3\varphi_1}{\partial x\,\partial t^2}-\right.$$
$$c_1^2m_6\left(\frac{\partial^3\varphi_1}{\partial x\,\partial t^2}+\frac{\partial^4 w_1}{\partial x^2\partial t^2}\right)+mf_0V_{mf}\frac{\partial^2 u_1}{\partial x\,\partial t}\sin\theta-mf_0V_{mf}\frac{\partial u_1}{\partial t}\frac{\partial^2 w_1}{\partial x^2}\cos\theta+c_1mf_4\frac{\partial^3\varphi_1}{\partial x\,\partial t^2}-c_1^2mf_6\frac{\partial^3\varphi_1}{\partial x\,\partial t^2}-$$
$$c_1^2mf_6\frac{\partial^4 w_1}{\partial x^2\partial t^2}+2mf_0V_{mf}\frac{\partial^2 w_1}{\partial x\,\partial t}\cos\theta+mf_0V_{mf}\frac{\partial w_1}{\partial t}\frac{\partial^2 w_1}{\partial x^2}\sin\theta+4k_ww_1-4G_p\frac{\partial^2 w_1}{\partial x^2}-k_ww_2+G_p\frac{\partial^2 w_2}{\partial x_2}- \tag{28}$$
$$c_v\frac{\partial w_2}{\partial t}-c_v\frac{\partial w_1}{\partial t}+mf_0V_{mf}{}^2\frac{\partial^2 w_1}{\partial x^2}\cos\theta+2\eta AH_x^2\frac{\partial^2 w_1}{\partial x^2}-\mu_eA_fV_{mf}\frac{\partial^3 w_1}{\partial x^3}-$$
$$\left.\mu_eA_fV_{mf}\frac{\partial^3 w_1}{\partial x^2\partial t}-\mu_eA_fV_{mf}\left(\frac{\partial^2 w_1}{\partial x^2}\right)^2\sin\theta\right]=0$$

where in these equations:

$$(m_{f0},m_{f1},m_{f2},m_{f4},m_{f6})=\rho_f\int(1,z,z^2,z^4,z^6)dA\ ,\ \ (m_0,m_1,m_2,m_4,m_6)=\rho_t\int(1,z,z^2,z^4,z^6)dA$$
$$\hat{I}=I-C_1J\ ,\ \hat{J}=J-C_1K\ ,\ \hat{m}_2=m_2-C_1m_4\ ,\ \hat{m}_4=m_4-C_1m_6\ ,\ \tilde{A}=\bar{A}-C_2I\ ,\ \bar{A}=A-C_2J \tag{29}$$

It should be noted that for the secondary nanotube, these equations are valid except that the indices of number "1" must be replaced with number "2" and vice versa.

We can define the dimensionless parameters as follows:

$$\xi=\frac{x}{L}\ ,\ (w_i,u_i)=\frac{(w_i,u_i)}{r}\ ,\ \eta_i=\frac{L}{r_i}\ ,\ en=\frac{e_0a}{L}\ ,\ \tau=\frac{t}{L}\sqrt{\frac{E}{\rho_t}}\ ,\ u_{mf}=\sqrt{\frac{\rho_f}{E}}V_{mf}\ ,\ \bar{\mu}_e=\frac{\mu_e}{r\sqrt{E\,\rho_f}}\ ,\ f_i=\frac{A_f}{A_i}\ ,$$
$$\bar{\rho}=\frac{\rho_f}{\rho_t}\ ,\ \bar{\varphi}=\varphi\ ,\ \bar{k}_w=\frac{k_wL^2}{EA}\ ,\ \bar{G}_p=\frac{G_p}{EA}\ ,\ \beta=\frac{K_sGA}{EA}\ ,\ \bar{\bar{I}}=\frac{c_1\hat{J}}{\hat{I}}\ ,\ \bar{G}=\frac{G}{E}\ ,\ \overset{0}{I}=\frac{\tilde{A}L^2}{\hat{I}}\ ,\ \overset{0}{m}=\frac{\hat{m}_2}{\rho_t\hat{I}}\ ,\ I^*=\frac{I_f}{\hat{I}}\ ,$$
$$I^n=\frac{C_1J}{\hat{I}}\ ,\ \breve{I}=\frac{C_1^2K}{\hat{I}}\ ,\ I^m=\frac{C_1\hat{m}_4}{\rho_t\hat{I}}\ ,\ \overset{0}{A}=\frac{A_t}{\tilde{A}}\ ,\ A^*=\frac{A_f}{\tilde{A}}\ ,\ \tilde{K}_w=\frac{K_wL^2}{G\tilde{A}}\ ,\ \tilde{G}_P=\frac{G_P}{G\tilde{A}}\ ,\ \bar{u}_{mf}=\sqrt{\frac{\rho_f}{G}}V_{mf}\ , \tag{30}$$
$$S=\frac{V_{mf}\,\mu_e}{LG}\ ,\ \tilde{\mu}_e=\frac{\mu_e}{L\sqrt{E\,\rho_t}}\ ,\ j^*=\frac{C_1J}{rL\tilde{A}}\ ,\ K^*=\frac{C_1^2K}{rL\tilde{A}}\ ,\ MP=\frac{\eta^mH_x{}^2}{G}\ ,\ \bar{C}=\frac{C_VL}{\tilde{A}\sqrt{\rho_tE}}\ ,\ I'=\frac{C_1J}{I}$$

According to the above relations, the dimensionless motion equations can be rewritten as:

δu_1:

$$\frac{\partial^2 u_1}{\partial \xi^2}-(\bar{\rho}f_1+1)\frac{\partial^2 u_1}{\partial \tau^2}+(en)^2(1+\bar{\rho}f_1)\frac{\partial^4 u_1}{\partial \xi^2\partial \tau^2}+\sqrt{\bar{\rho}}f_1 u_{mf}\ \frac{1}{\eta}\frac{\partial^2 w_1}{\partial \xi\partial \tau}\frac{\partial w}{\partial \xi}-(en)^2\sqrt{\bar{\rho}}fu_{mf}\ \frac{1}{\eta}\frac{\partial^4 w_1}{\partial \xi^3\partial \tau}\frac{\partial w}{\partial \xi}-$$
$$(en)^2\sqrt{\bar{\rho}}fu_{mf}\ \frac{1}{\eta}\frac{\partial^2 w_1}{\partial \xi\partial \tau}\frac{\partial^3 w_1}{\partial \xi^3}+(en)^2\sqrt{\bar{\rho}}fu_{mf}\left(\frac{1}{\eta}\right)^3\frac{\partial^2 w_1}{\partial \xi\partial \tau}\left(\frac{\partial^2 w_1}{\partial \xi^2}\right)^2\frac{\partial w}{\partial \xi}-2(en)^2\sqrt{\bar{\rho}}fu_{mf}\ \frac{1}{\eta}\frac{\partial^3 w}{\partial \xi^2\partial \tau}\frac{\partial^2 w}{\partial \xi^2}+$$
$$\frac{1}{\eta}u_{mf}{}^2 f\ \frac{\partial^2 w}{\partial \xi^2}\frac{\partial w}{\partial \xi}-(en)^2 fu_{mf}{}^2\frac{1}{\eta}\frac{\partial^4 w}{\partial \xi^4}\frac{\partial w}{\partial \xi}-3(en)^2 fu_{mf}{}^2\frac{1}{\eta}\frac{\partial^2 w}{\partial \xi^2}\frac{\partial^3 w}{\partial \xi^3}+(en)^2 fu_{mf}{}^2\left(\frac{1}{\eta}\right)^3\left(\frac{\partial^2 w}{\partial \xi^2}\right)^3\frac{\partial w}{\partial \xi}+ \qquad (31)$$
$$\bar{\mu}\sqrt{\bar{\rho}}f\ \frac{1}{\eta}\frac{\partial^3 u}{\partial \xi^2\partial \tau}-(en)^2\sqrt{\bar{\rho}}\bar{\mu}f\ \frac{1}{\eta}\frac{\partial^5 u}{\partial \xi^4\partial \tau}+f\ \bar{\mu}u_{mf}\left(\frac{1}{\eta}\right)^2\left[-\frac{\partial^3 w}{\partial \xi^3}\frac{\partial w}{\partial \xi}+(en)^2\frac{\partial^5 w}{\partial \xi^5}\frac{\partial w}{\partial \xi}+3(en)^2\left(\frac{\partial^3 w}{\partial \xi^3}\right)^2-\right.$$
$$\left.6(en)^2\left(\frac{1}{\eta}\right)^2\frac{\partial^3 w}{\partial \xi^3}\left(\frac{\partial^2 w}{\partial \xi^2}\right)^2\frac{\partial w}{\partial \xi}+4(en)^2\frac{\partial^4 w}{\partial \xi^4}\frac{\partial^2 w}{\partial \xi^2}-\left(\frac{\partial^2 w}{\partial \xi^2}\right)^2-(en)^2\left(\frac{1}{\eta}\right)^2\left(\frac{\partial^2 w}{\partial \xi^2}\right)^4\right]$$

$\delta\varphi_1$:

$$\frac{\partial^2 \varphi}{\partial \xi^2}-\bar{\bar{I}}\left(\frac{\partial^2 \varphi}{\partial \xi^2}+\frac{1}{\eta}\frac{\partial^3 w}{\partial \xi^3}\right)-\bar{G}I^{\circ}\left(\varphi+\frac{1}{\eta}\frac{\partial w}{\partial \xi}\right)-\overset{\circ}{m}\frac{\partial^2 \varphi}{\partial \tau^2}+I^m\left(\frac{\partial^2 \varphi}{\partial \tau^2}+\frac{1}{\eta}\frac{\partial^3 w}{\partial \xi\partial \tau^2}\right)-\bar{\rho}I^*\frac{\partial^2 \varphi}{\partial \tau^2}$$
$$+\bar{\rho}I^n\left(2\frac{\partial^2 \varphi}{\partial \tau^2}+\frac{1}{\eta}\frac{\partial^3 w}{\partial \xi\partial \tau^2}\right)-\bar{\rho}\breve{I}\left(\frac{\partial^2 \varphi}{\partial \tau^2}+\frac{1}{\eta}\frac{\partial^3 w}{\partial \xi\partial \tau^2}\right)+(en)^2\left[\overset{0}{m}\frac{\partial^4 \varphi}{\partial \xi^2\partial \tau^2}-I^m\left(\frac{\partial^4 \varphi}{\partial \xi^2\partial \tau^2}+\frac{1}{\eta}\frac{\partial^5 w}{\partial \xi^3\partial \tau^2}\right)\right. \qquad (32)$$
$$\left.+\bar{\rho}I^*\frac{\partial^4 w}{\partial \xi^2\partial \tau^2}-\bar{\rho}I^n\left(-2\frac{\partial^4 \varphi}{\partial \xi^2\partial \tau^2}+\frac{1}{\eta}\frac{\partial^5 w}{\partial \xi^3\partial \tau^2}\right)-\bar{\rho}\breve{I}\left(\frac{\partial^4 \varphi}{\partial \xi^2\partial \tau^2}+\frac{1}{\eta}\frac{\partial^5 w}{\partial \xi^3\partial \tau^2}\right)\right]$$

δw_1:

$$\frac{\partial^2 w}{\partial \xi^2}+\eta\frac{\partial \varphi}{\partial \xi}+\frac{1}{\bar{\bar{G}}}\frac{\partial^3 \varphi}{\partial \xi^3}\left(J^*-K^*\right)-\frac{1}{\bar{\bar{G}}\eta}K^*\frac{\partial^4 w}{\partial \xi^4}-\frac{1}{\bar{\bar{G}}}\overset{\circ}{A}\frac{\partial^2 w}{\partial \tau^2}+\frac{1}{\bar{\bar{G}}}\frac{\partial^3 \varphi}{\partial \xi\partial \tau^2}\left(K^*-J^*\right)+\frac{1}{\bar{\bar{G}}\eta}K^*\frac{\partial^4 w}{\partial \xi^2\partial \tau^2}+(en)^2\frac{1}{\bar{\bar{G}}}\left[\overset{\circ}{A}\frac{\partial^4 w}{\partial \xi^2\partial \tau^2}+J^*\frac{\partial^5 \varphi}{\partial \xi^3\partial \tau^2}-\right.$$
$$K^*\frac{\partial^5 \varphi}{\partial \xi^3\partial \tau^2}-\frac{1}{\eta}K^*\frac{\partial^6 w}{\partial \xi^4\partial \tau^2}+A^*u_{mf}\sqrt{\rho}\left(\frac{1}{\eta}\right)\left(-\frac{\partial^4 u_1}{\partial \xi^3\partial \tau}\frac{\partial w}{\partial \xi}+3\frac{\partial^2 w}{\partial \xi^2}\frac{\partial^3 u}{\partial \xi^2\partial \tau}+3\frac{\partial^3 w}{\partial \xi^3}\frac{\partial^2 u}{\partial \xi\partial \tau}+3\left(\frac{1}{\eta}\right)^2\left(\frac{\partial^2 w}{\partial \xi^2}\right)^2\left(\frac{\partial^2 u}{\partial \xi\partial \tau}\right)\frac{\partial w}{\partial \xi}-\frac{\partial u}{\partial \tau}\frac{\partial^4 u}{\partial \xi^4}+\right.$$
$$3\left(\frac{1}{\eta}\right)^2\frac{\partial u}{\partial \tau}\frac{\partial^2 w}{\partial \xi^2}\frac{\partial^3 w}{\partial \xi^3}\frac{\partial w}{\partial \xi}+\left(\frac{1}{\eta}\right)^2\left(\frac{\partial^2 w}{\partial \xi^2}\right)^3\frac{\partial u}{\partial \tau}\Bigg)+\bar{\rho}J^*\frac{\partial^5 \varphi}{\partial \xi^3\partial \tau^2}-\bar{\rho}K^*\frac{\partial^5 \varphi}{\partial \xi^3\partial \tau^2}-\bar{\rho}\frac{K^*}{\eta}\frac{\partial^6 w}{\partial \xi^4\partial \tau^2}+\bar{\rho}A^*\frac{\partial^4 w}{\partial \xi^2\partial \tau^2}+$$
$$A^*\sqrt{\rho}u_{mf}\left(2\frac{\partial^4 w}{\partial \xi^3\partial \tau}+\left(\frac{1}{\eta}\right)^2\left(-5\frac{\partial^2 w}{\partial \xi^2}\frac{\partial^3 w}{\partial \xi^2\partial \tau}\frac{\partial w}{\partial \xi}-4\frac{\partial^3 w}{\partial \xi^3}\frac{\partial^2 w}{\partial \xi\partial \tau}\frac{\partial w}{\partial \xi}-4\left(\frac{\partial^2 w}{\partial \xi^2}\right)^2\frac{\partial^2 w}{\partial \xi\partial \tau}-\frac{\partial w}{\partial \tau}\frac{\partial^4 w}{\partial \xi^4}\frac{\partial w}{\partial \xi}-\frac{\partial^2 w}{\partial \xi^2}\frac{\partial w}{\partial \tau}\frac{\partial^3 w}{\partial \xi^3}-\right.\right.$$
$$\left.\left.2\left(\frac{\partial^3 w}{\partial \xi^3}\right)\left(\frac{\partial^2 w}{\partial \xi^2}\right)\left(\frac{\partial w}{\partial \tau}\right)\right)\right)+\sqrt{\rho}u_{mf}\left(\frac{1}{\eta}\right)^4\left(\frac{\partial^2 w}{\partial \xi^2}\right)^3\frac{\partial w}{\partial \tau}\frac{\partial w}{\partial \xi}\Bigg]+(en)^2\left[4\tilde{k}_w\frac{\partial^2 w_1}{\partial \xi^2}-4\tilde{G}_p\frac{\partial^4 w_1}{\partial \xi^4}-\tilde{k}_w\frac{\partial^2 w_2}{\partial \xi^2}+\tilde{G}_p\frac{\partial^4 w_2}{\partial \xi^4}-\right. \qquad (33)$$
$$\frac{1}{\bar{\bar{G}}}\bar{C}\left(\frac{\partial^3 w_1}{\partial \xi^2\partial \tau}+\frac{\partial^3 w_2}{\partial \xi^2\partial \tau}\right)+A^*u_{mf}^2\left(\frac{\partial^4 w}{\partial \xi^4}-3\left(\frac{1}{\eta}\right)^2\frac{\partial^2 w}{\partial \xi^2}\frac{\partial^3 w}{\partial \xi^3}\frac{\partial w}{\partial \xi}-\left(\frac{1}{\eta}\right)^2\left(\frac{\partial^2 w}{\partial \xi^2}\right)^3\right)-2(MP)\overset{\circ}{A}\frac{\partial^4 w}{\partial \xi^4}A^*S\left(-\frac{\partial^5 w}{\partial \xi^5}+\right.$$
$$2\left(\frac{1}{\eta}\right)^2\left(\frac{\partial^2 w}{\partial \xi^2}\right)\left(\frac{\partial^4 w}{\partial \xi^4}\right)\frac{\partial w}{\partial \xi}+\left(\frac{\partial^2 w}{\partial \xi^2}\right)^2\left(\frac{\partial^3 w}{\partial \xi^3}\right)+\left(\frac{1}{\eta}\right)^2\left(\frac{\partial^3 w}{\partial \xi^3}\right)^2\frac{\partial w}{\partial \xi}+2\left(\frac{1}{\eta}\right)^2\left(\frac{\partial^4 w}{\partial \xi^4}\right)\left(\frac{\partial^2 w}{\partial \xi^2}\right)\frac{\partial w}{\partial \xi}+2\left(\frac{1}{\eta}\right)^2\left(\frac{\partial^3 w}{\partial \xi^3}\right)\frac{\partial w}{\partial \xi}+$$
$$\left.5\left(\frac{1}{\eta}\right)^2\left(\frac{\partial^3 w_1}{\partial \xi^3}\right)\left(\frac{\partial^2 w_1}{\partial \xi^2}\right)^2-\left(\frac{1}{\eta}\right)^4\left(\frac{\partial^2 w}{\partial \xi^2}\right)^4\frac{\partial w_1}{\partial \xi}\right)-A^*\frac{1}{\bar{\bar{G}}}\tilde{\mu}_e\frac{\partial^5 w_1}{\partial \xi^4\partial \tau}\Bigg]+A^*\left(\frac{1}{\eta}\right)\frac{1}{\bar{\bar{G}}}\sqrt{\rho}u_{mf}\left(\frac{\partial^2 u_1}{\partial \xi\partial \tau}\frac{\partial w_1}{\partial \xi}+\frac{\partial u_1}{\partial \tau}\frac{\partial^2 w_1}{\partial \xi^2}\right)+$$
$$\frac{\bar{\bar{\rho}}}{\bar{\bar{G}}}\left(-J^*\frac{\partial^3 \phi}{\partial \xi\partial \tau^2}+K^*\frac{\partial^3 \varphi}{\partial \xi\partial \tau^2}\frac{K^*}{\eta}\frac{\partial^4 w_1}{\partial \xi^2\partial \tau^2}-A^*\frac{\partial^2 w_1}{\partial \tau^2}\right)+\sqrt{\rho}u_{mf}A^*\frac{1}{\bar{\bar{G}}}\left(-2\frac{\partial^2 w_1}{\partial \xi\partial \tau}+\left(\frac{1}{\eta}\right)^2\frac{\partial w_1}{\partial \tau}\frac{\partial^2 w_1}{\partial \xi^2}\frac{\partial w_1}{\partial \xi}\right)-4\tilde{k}_w w_1+$$
$$4\tilde{G}_p\frac{\partial^2 w_1}{\partial \xi^2}+\tilde{k}_w w_2-\tilde{G}_p\frac{\partial^2 w_2}{\partial \xi^2}+\frac{\bar{\bar{C}}}{\bar{\bar{G}}}\left(\frac{\partial w_1}{\partial \tau}+\frac{\partial w_2}{\partial \tau}\right)-A^*\bar{u}_{mf}\frac{\partial^2 w}{\partial \xi^2}+A^*S\left(\frac{\partial^3 w_1}{\partial \xi^3}-\left(\frac{1}{\eta}\right)^2\left(\frac{\partial^2 w_1}{\partial \xi^2}\right)^2\frac{\partial w_1}{\partial \xi}\right)+\frac{A^*}{\bar{\bar{G}}}\tilde{\mu}_e\frac{\partial^3 w_1}{\partial \xi^2\partial \tau}-2(MP)\overset{\circ}{A}\frac{\partial^2 w_1}{\partial \xi^2}=0$$

For the secondary nanotube, these equations are valid except that the indices of number "1" must be replaced with number "2" and vice versa.

4. Solution Method

In this investigation a numerical method, namely the DQ approach, is used to solve the higher-order equations of motion. In this method, the partial derivative of a function with respect to the spatial variables at a given discrete point are approximated as a weighted linear combination of the function values at all the discrete points chosen in the solution domain. Accordingly, the *n*th partial derivative of the functions u_i, v_i and w_i are approximated as [16]:

$$\frac{\partial^n}{\partial \zeta^n}\left\{u_i, v_i, w_i\right\}\Big|_{\zeta=\zeta_i} = C_{jm}^{(n)}\left\{u_{im}(\zeta,t), v_{im}(\zeta,t), w_{im}(\zeta,t)\right\}, \quad i=1,2 \ , \ m=1,2,...,N \tag{34}$$

where the summation convention is used for the dummy index m, N is the number of grid points along the nanotubes and $C_{jm}^{(n)}$ represents the Lagrange interpolation polynomial and its *k*th derivative, which can be found in [17]. An assumption of the solution of Equations (26-28) can be seen as [18]:

$$u_i(x,t) = u_i(x)e^{\omega\tau} \tag{35a}$$

$$\varphi_i(x,t) = \varphi_i(x)e^{\omega\tau} \tag{35b}$$

$$w_i(x,t) = w_i(x)e^{\omega\tau} \tag{35c}$$

where $\omega = \lambda h\sqrt{\rho_f / E}$ is the dimensionless natural frequency, λ is the (fundamental) natural frequency. The DQ form of the clamped boundary conditions at both ends of the nanotubes may be written in a dimensionless form as:

$$\begin{aligned} &u_{i1} = v_{i1} = w_{i1} = 0 \ , \ C_{2m}^{(1)} w_{im} = 0 \ , \ \text{at}\ \zeta = 0 \\ &u_{iN} = v_{iN} = w_{iN} = 0 \ , \ C_{N-1m}^{(1)} w_{im} = 0 \ , \ \text{at}\ \zeta = 1 \\ &m = 1,2,...,N \end{aligned} \tag{36}$$

Applying the above boundary conditions to Equations (31-33) leads to the following matrix equation:

$$\left([K] + \omega[C] + \omega^2[M]\right)\begin{pmatrix} d_b \\ d_d \end{pmatrix} = 0 \tag{37}$$

where the subscript *b* stands for the elements related to the boundary points whereas subscript *d* is associated with the remainder elements. $[K], [C]$ and $[M]$ are the stiffness, damping and mass matrices, respectively. To solve Equation (37) and reduce it to the standard form of the eigenvalue problem, it is convenient to rewrite it as the following first order variable as [16]:

$$\{\dot{Z}\} = [A]\{Z\} \tag{38}$$

in which the state vector Z and the state space matrix $[A]$ are defined as:

$$Z = \begin{Bmatrix} d_a \\ \dot{d}_a \end{Bmatrix}, \ [A] = \begin{bmatrix} [0] & [I] \\ -\left[M^{-1}K\right] & -\left[M^{-1}C\right] \end{bmatrix} \tag{39}$$

where $[0]$ and $[I]$ are the zero and unity matrices, respectively. However, the frequencies obtained from the solution of Equation (38) are complex due to damping. Hence, the results contain two real and imaginary parts. The real part corresponds to the system damping and the imaginary part represents the system's natural frequencies.

5. Numerical Results and Discussion

In this paper, the instability and vibration of a coupled CNT system conveying a viscose fluid under a magnetic field and surrounded by a Visco-Pasternak foundation is investigated. In the following figures, the effect of different parameters such as small scale, elastic medium, Knudsen number and magnetic field on the dimensionless frequency and stability of the system is investigated. The mechanical and geometrical properties of CNT are considered as:

$$\begin{aligned} &\mathrm{E} = 1\,\mathrm{TPa} \ , \ \rho_t = 2300\frac{\mathrm{Kg}}{\mathrm{m}^3} \ , \ \rho_f = 1000\frac{\mathrm{Kg}}{\mathrm{m}^3} \\ &\mathrm{r_1} = \mathrm{r_2} = 0.5\,\mathrm{nm} \ , \ \mathrm{t} = 0.34\,\mathrm{nm} \ , \ \upsilon = 0.2 \end{aligned} \tag{40}$$

To validate the results of this study, Figure 2 is presented to compare with Reference [19] in which, a simplified case of this study is carried out by considering Timoshenko's displacement field, and neglecting the magnetic field and the Knudsen number. This figure demonstrates that there is a good agreement between these two studies.

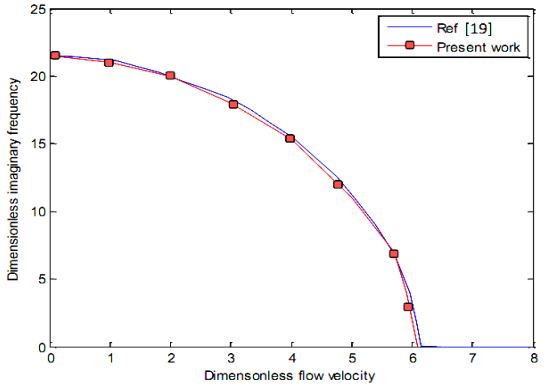

Fig. 2. A comparison between the results of this study and Ref. [19]

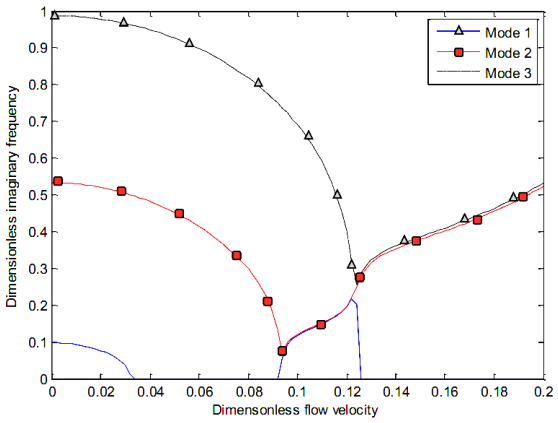

Fig. 3a. Dimensionless imaginary part of the frequencies versus the dimensionless flow velocity

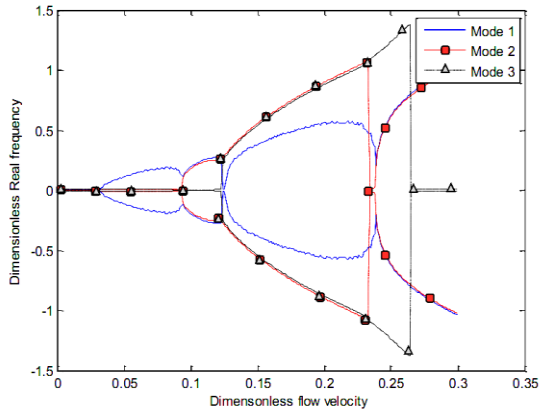

Fig. 3b. Dimensionless real part of the frequencies versus the dimensionless flow velocity

The dimensionless imaginary and real frequencies versus the dimensionless flow velocity for various modes of vibration are depicted in Figures 3a and 3b. It must be noted that *Im*(ω)represents the resonance frequencies of the system, while $\mathrm{Re}(\omega)$ denotes the damping ones. As shown in these figures, with increasing fluid velocity, the imaginary part of the frequency decreases while the real part remains at zero until $\mathrm{Im}(\omega)$ drops to zero, while $\mathrm{Re}(\omega)$ starts to ascend. This velocity of the fluid is called CFV. For the velocities less than CFV, the system remains stable and this range of fluid velocity is safe for design purposes. In the vicinity of CFV up to 0.092, $\mathrm{Im}(\omega)$ remains at zero and a coupled system becomes unstable. When the fluid velocity increases beyond 0.092, a flutter phenomenon occurs, whereby two vibration modes merge. Flutter conditions must be avoided because these are dangerous for the system. By increasing the flow velocity the sequence of divergence, flutter and stable behaviours occurs again. The same behaviour can also be observed for other vibration modes.

The variations of dimensionless imaginary frequencies versus dimensionless fluid velocities for various values of the aspect ratio (L/r) are shown in Figure 4. It is obvious that the imaginary part of the frequency decreases with an increase in the aspect ratio. Moreover, as L/r decreases, the CFV increases. Therefore, the low aspect ratio should be taken into account for coupled CNTs system in an optimum design of nano/micro devices.

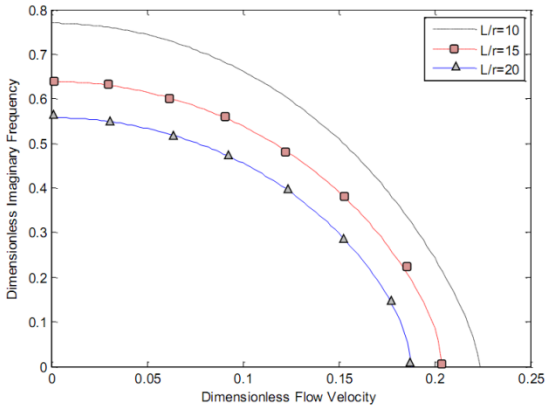

Fig. 4. Dimensionless imaginary frequency against velocity for various values of aspect ratio

Figure 5 shows the imaginary part of the dimensionless frequency versus the flow velocity for different values of small scale. It is obvious that the nonlocal parameter is a significant parameter in the vibration of the coupled system. As can be seen, increasing the nonlocal

parameter alleviates the frequency and CFV. It must be noted that the zero value for nonlocal parameters (i.e., $e_0 a = 0$) denotes the result obtained by the classical Reddy beam model which has the highest frequency and CFV.

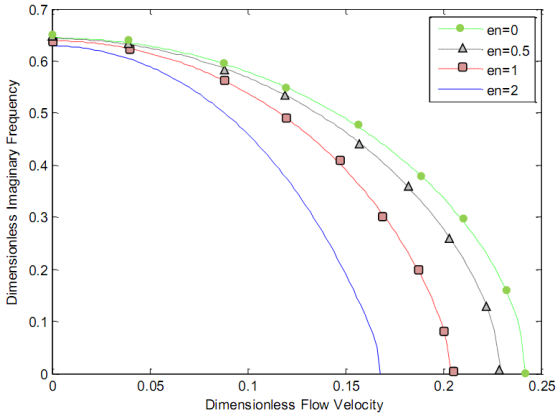

Fig. 5. Dimensionless natural frequency dimensionless flow velocity for different values of small scale parameters

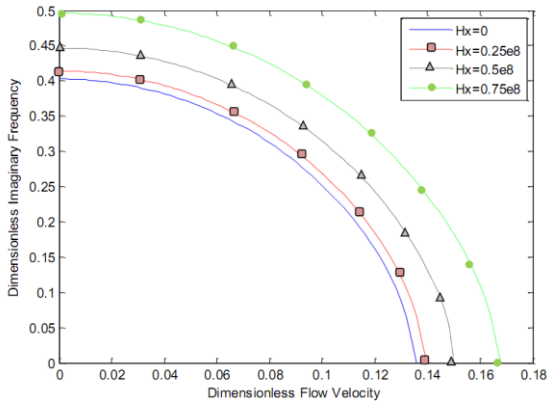

Fig 6. Effect of magnetic field intensity on the natural frequency of a coupled system

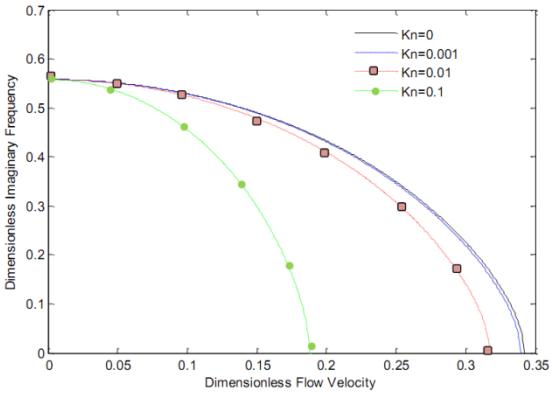

Fig. 7. Effect of the Knudsen number on the dimensionless imaginary frequency

The effect of the magnetic field on the dimensionless frequency of the coupled CNTs is shown in Figure 6. As already mentioned, applying a magnetic field in the axial direction generates a force in the radial direction that is called the Lorentz force. It is concluded that the frequency and CFV increase with an increase in the magnetic intensity. Regarding the Lorentz force effect, it is evident that the magnetic field is an effective factor in increasing resonance frequency, leading to the stability of the system.

The variation of the natural frequency with respect to the fluid velocity for different values of the Knudsen number is illustrated in Figure 7. The Knudsen number is defined based on various flow regimes. Here, the slip flow regime is considered. As shown in these figures, the continuum fluid (*Kn=0*) predicts the highest frequency zone, considering a fluid with a higher Knudsen number results in shifting the curves to the lower frequency region. Therefore, the critical flow velocity of the coupled system decreases with increasing Kn.

Figure 8 indicates that the existence of a spring foundation enlarges the stability region of the coupled system and increases the resonance frequency. Since the Winkler modulus is equal in the whole coupled system, the abovementioned figure shows the effect of this spring modulus which is located at parties and is between CNTs. The results illustrate that the $\mathrm{Im}(\omega)$ increases with the increasing Winkler module and decreases as U_{mf} increases.

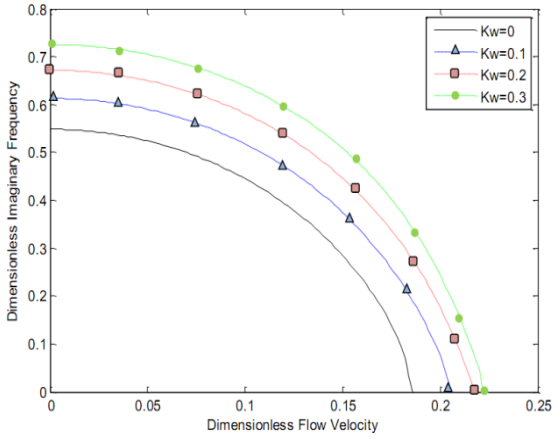

Fig. 8. Effect of the modulus of the Winkler foundation on the dimensionless natural frequency versus the dimensionless flow velocity

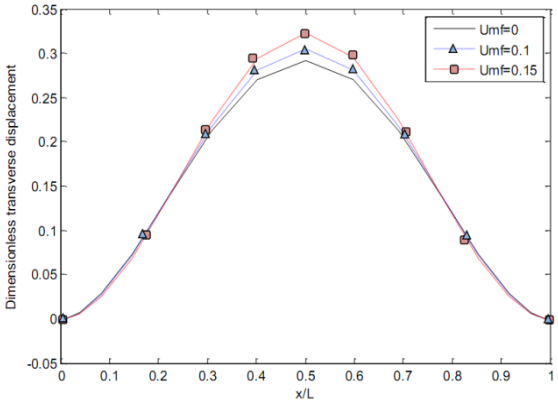

Fig. 9. Dimensionless transverse displacement along nanotubes for three different values of the dimensionless fluid velocity for the in-phase mode

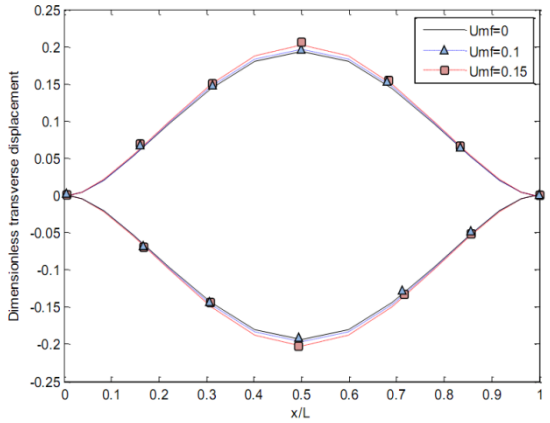

Fig. 10. Dimensionless transverse displacement along nanotubes for three different values of dimensionless fluid velocity for the out-of-phase mode

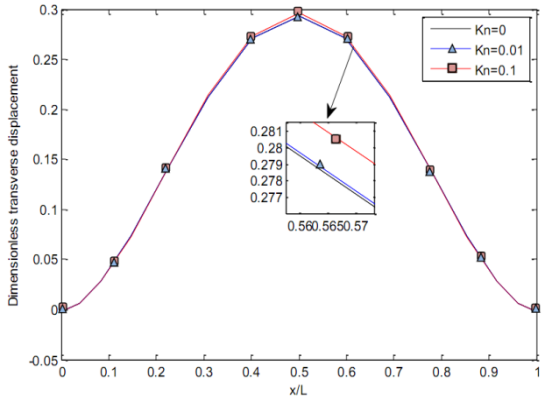

Fig. 11. Effect of the Knudsen number on transverse displacement along the nanotube

Transverse displacements of a coupled system for an in-phase state are demonstrated in Figure 9. As can be predicted, the mode shape of both CNTs is of equal quantity and direction. Moreover, increasing the velocity of the fluid leads to increasing transverse displacements. In addition, the clamp-clamp boundary conditions are satisfied at both ends of the nanotubes where the deflection and slop are zero.

Figure 10 illustrates the distribution of the out-of-phase transverse displacement along the nanotubes with varying fluid velocity. In the out-of-phase mode, the transverse displacement directions of each CNT are opposite. Furthermore, increasing flow velocity causes an increase in the magnitude of transverse displacements. Furthermore, similar to Figure 9, it is found that the transverse displacements are zero at both ends of the nanotubes due to the assumed boundary conditions.

Figure 11 shows the transverse displacement for the in-phase state versus the dimensionless nanotube length with a varying Knudsen number. As can be seen in this figure, with an increasing Knudsen number the transverse displacement increases.

5. Conclusion

In this study, the nonlinear vibration and stability of double CNTs conveying viscose fluid in a Visco-Pasternak foundation were investigated. A uniform magnetic field is applied to the system. The nonlinear higher-order equations of motion were obtained using Hamilton's principle. The DQ method was utilized to solve these equations. Here are some of the conclusions that can be drawn from the results:

1. Considering fluid flow, it can be concluded that fluid flow and velocity are effective parameters for decreasing natural frequency, resulting in the instability of the system.

2. The stability of the system depends strongly on nanotube length so that increasing the length of the nanotube leads to a decreasing stability region.

3. The magnetic field has the same effect as the length of the nanotube, whereby the magnetic field intensity increases as the stability region of the system decreases.

4. As the surrounding medium is stiffer, the stability of the system increases.

5. Increasing the small scale parameter decreases the system's stability.

Acknowledgement

The author would like to thank the reviewers for their valuable comments and suggestions to improve the clarity of this study. The authors are grateful to University of Kashan for supporting this work by Grant No. 363443/35. They would also like to thank the Iranian Nanotechnology Development Committee for their financial support."

References

[1].Reddy J.N., 2007, Nonlocal theories for bending, buckling and vibration of beams, Int. J. Sci. Technol. **45**: 288-307.

[2].Reddy J. N., Wang C. M., 2004, Dynamics of fluid-conveying beams, Centre for Offshore Research and Engineering, National University of Singapore, CORE Report: 1-21.

[3].Wang L., Ni Q., 2008, On vibration and instability of carbon nanotubes conveying fluid, Comput. Mater. Sci. **43**: 399-402.

[4].Chang T.P., 2012, Thermal-mechanical vibration and instability of a fluid-conveying single-walled carbon nanotubes embedded in an elastic medium based on nonlocal elasticity theory, Appl. Math. Modell. **36**: 1964-1973.

[5].Ghorbanpour Arani A., Zarei M. Sh., Amir S., Khoddami Maraghi Z., 2013, nonlinear nonlocal vibration embedded DWCNT conveying fluid using shell model, Physica B. **410**: 188-196.

[6].GhorbanpourArani A., Amir S., 2014, Electro-thermal vibration of visco-elastically coupled BNNT systems conveying fluid embedded on elastic foundation via strain gradient theory, Physica B. **419**: 1–6.

[7].Murmu T., Adhikari S., 2011, Axial instability of double-nanobeam-systems, Phys. Lett. A. **375**: 601-608.

[8].Simsek M., 2011, Nonlocal effects in the forced vibration of an elastically connected double-carbon nanotube system under a moving nanoparticle, Comput. Mater. Sci. **50**: 2112-2123.

[9].Murmu T., Adhikari S., 2012, Nonlocal elasticity based vibration of initially pre-stressed coupled nanobeam systems, Eur. J. Mech. A. Solids **34**: 52-62.

[10]. Kuang Y.D., He X.Q., Chen C.Y., Li G.Q., 2009, Analysis of nonlinear vibrations of double-walled carbon nanotubes conveying fluid, Comput. Mater. Sci. **45**: 745-756.

[11]. Wang H., Dong K., Men F., Yan Y.J., Wang X., 2010, Influences of longitudinal magnetic field on wave propagation in carbon nanotubes embedded in elastic matrix, Appl. Math. Modell. **34**: 878-889.

[12]. Wang L., Ni Q, 2009, A reappraisal of the computational modelling of carbon nanotubes conveying viscose fluid, Mech. Res. Commun. **36**: 833-837.

[13]. Beskok A., Karniadakis G.E., 1999, A model for flows in channels, pipes and ducts at micro and nano scale, Microscale Thermophys. Eng. **3**: 43-77.

[14]. Rashidi V., Mirdamadi H.R., Shirani E., 2012, A novel model for vibrations of nanotubes conveying nanoflow, Comput. Mater. Sci. **51**: 347-352.

[15]. Eringen A.C., 1983, On differential equations of nonlocal elasticity and solutions of screw dislocation and surface waves, J. Appl. Phys. **54**: 4703- 4710.

[16]. Ke L.L., Wang Y.Sh., 2011, Flow-induced vibration and instability of embedded double-walled carbon nanotubes based on a modified couple stress theory, Physica E. **43**: 1031-1039.

[17]. Karami G., Malekzadeh P., 2002, A new differential quadrature methodology for beam analysis and the associated differential quadrature element method, Comput. Methods Appl. Mech. Eng. **191**: 3509-3526.

[18]. Ke L.L., Xiang Y., Yang J., Kitipornchai S., 2009, Nonlinear free vibration of embedded double-walled carbon nanotubes based on nonlocal Timoshenko beam theory, Comput. Mater.Sci. **47**: 409-417.

[19]. Chang W. J., Lee H. L., 2009, Free vibration of a single-walled carbon nanotube containing a fluid flow using the Timoshenko beam model, Phys. Lett. A. **373**: 982-985.